Solar Phys (2008) 251: 627–639
DOI 10.1007/s11207-008-9140-9

Mechanics of Seismic Emission from Solar Flares

C. Lindsey · A.-C. Donea

Received: 16 October 2007 / Accepted: 5 February 2008 / Published online: 22 March 2008

Abstract Instances of seismic transients emitted into the solar interior in the impulsive phases of some solar flares offer a promising diagnostic tool, both for understanding the physics of solar flares and for the general development of local helioseismology. Among the prospective contributors to flare acoustic emission that have been considered are: *i*) chromospheric shocks propelled by pressure transients caused by impulsive thick-target heating of the upper and middle chromosphere by high-energy particles, *ii*) heating of the photosphere by continuum radiation from the chromosphere or possibly by high-energy protons, and *iii*) magnetic-force transients caused by magnetic reconnection. Hydrodynamic modeling of chromospheric shocks suggests that radiative losses deplete all but a small fraction of the energy initially deposited into them before they penetrate the photosphere. Comparisons between the spatial distribution of acoustic sources, derived from seismic holography of the surface signatures of flare acoustic emission, and the spatial distributions of sudden changes both in visible-light emission and in magnetic signatures offer a possible means of discriminating between contributions to flare acoustic emission from photospheric heating and magnetic-force transients. In this study we develop and test a means for estimating the seismic intensity and spatial distribution of flare acoustic emission from photospheric heating associated with visible-light emission and compare this with the helioseismic signatures of seismic emission. Similar techniques are applicable to transient magnetic signatures.

Keywords Flares, dynamics · Helioseismology

Helioseismology, Asteroseismology, and MHD Connections
Guest Editors: Laurent Gizon and Paul Cally

C. Lindsey (✉)
NorthWest Research Associates, Boulder, CO 80301, USA
e-mail: clindsey@cora.nwra.com

A.-C. Donea
Centre for Stellar and Planetary Astrophysics, School of Mathematical Sciences, Monash University, Melbourne, Victoria 3800, Australia
e-mail: alina.donea@sci.monash.edu.au

1. Introduction

Some solar flares are known to drive strong seismic transients into the subphotospheres of the magnetic regions that produce them (Kosovichev and Zharkova, 1998). These waves appear to be generated during the impulsive phase of the flare and usually emanate from a relatively compact region (Donea, Braun, and Lindsey, 1999; Donea and Lindsey, 2005). Most of this energy is refracted back to the solar surface within an hour of the onset of the flare, where it makes a surface ripple that can be discriminated by various techniques in local helioseismology. These "sunquakes" offer a powerful diagnostic of both the magnetohydrodynamics of seismic wave generation and propagation in the active-region chromosphere and photosphere and of the structure and dynamics of the active-region subphotosphere.

From a diagnostic point of view it can very well be argued that the discovery of seismic emission from flares is one of the most important developments in local helioseismology:

1. Flare acoustic transients represent the most localized coherent sources that we are aware of, temporally as well as spatially.
2. They are the "hardest" acoustic radiation known so far (*i.e.* the most intense at high frequencies).
3. They are the only acoustic waves that are known to be generated in plain view above the solar surface.

At the same time, there are significant unanswered questions about the physics of seismic emission from flares. For several years it appeared that flare acoustic emission was a relatively rare occurrence, the only known instance being that of the X2.6-class flare of 09 July 1996 discovered by Kosovichev and Zharkova (1998). However, a comprehensive survey by Donea *et al.* (2006a) uncovered more than a dozen instances of significant seismic transient emission in the declining phase of solar activity cycle 23, emanating from flares as small as class M6.7 (Martinez-Oliveros, Moradi, and Donea, 2000). This established that flare acoustic emission was a relatively common phenomenon. Some of these flares were observed by an impressive array of other space-borne and ground-based facilities. This has greatly increased diagnostic prospects of flare acoustic emission.

A number of mechanisms have been considered as possible contributors to flare acoustic emission:

1. Chromospheric shocks driven by sudden, thick-target heating of the upper and middle chromosphere (Kosovichev and Zharkova, 1995, 1998, 2006, 2007; Donea and Lindsey, 2005). Evidence of chromospheric shocks derived from chromospheric line profiles suggests that there is more than sufficient energy flux in the chromosphere to account for the energy seen in flare acoustic transients. However, hydrodynamic modeling of waves driven by thick-target heating of the chromosphere indicates that these waves are heavily damped by radiative losses, such that an insufficient amount of energy penetrates through the photosphere to explain the helioseismic observations (Fisher, Canfield, and McClymont, 1985; Ding and Fang, 1994; Allred *et al.*, 2005).
2. Wave-mechanical transients driven by heating of the photosphere. This contribution was initially suggested by Donea and Lindsey (2005), motivated by the strong spatial correspondence between sudden excess visible continuum emission emanating from active regions during the impulsive phases of flares and the source distributions of flare acoustic emission shown by seismic holography (Lindsey and Braun, 2000; Donea, Braun, and Lindsey, 1999; Donea and Lindsey, 2005) applied to helioseismic observations of the flares. Figure 1 shows an example. Seismic emission from flares has invariably emanated from within or near sunspot penumbrae in instances encountered

to date. The sources tend to be relatively compact (Donea, Braun, and Lindsey, 1999; Donea and Lindsey, 2005; Kosovichev, 2006) and are the site of sudden continuum emission as well as overlying chromospheric line emission. Considerable chromospheric line emission and significant continuum emission are seen from regions well outside of the seismic sources. However, as this study will confirm, the sudden, compact component of continuum emission is heavily concentrated in the region from which the high-frequency seismic emission emanates. Donea and Lindsey (2005), Donea *et al.* (2006b), and Moradi *et al.* (2007) suggested that the continuum emission is causally associated one way or another with photospheric heating, which would give rise to a pressure increase that would drive the acoustic transient. Once the transient penetrates substantially beneath the photosphere, significant radiative losses are supposed to be blocked by highly opaque ionized hydrogen, and the transient is supposed to proceed undamped until its next encounter with the solar surface.

3. Lorentz-force transients resulting from magnetic reconnection in the corona. Transient shifts in magnetic signatures have been detected in a number of flares, some of which were acoustically active and others of which were not (detectably). Zharkova and Kosovichev (2002) considered magnetic transients as a source of waves, both coronal, chromospheric and helioseismic, paying particular attention to magnetic observations of the flare of 14 July 2000. This flare was acoustically inactive as far as helioseismic analyses to date have been able to discern. Sudol and Harvey (2005) measured localized transients in the line-of-sight magnetic field in a variety of flares, including the acoustically active flare of 29 October 2003.[1] Donea *et al.* (2006b) found a strong local transient in the line-of-sight magnetic signature of the M9.5-class flare of 09 September 2001 coincident with the source region of strong transient acoustic emission. Hudson, Fisher, and Welsch (2008) have formally introduced the hypothesis that transient shifts in magnetic signatures during the impulsive phases of acoustically active flares are the result of flare-related magnetic reconnection and a source of flare acoustic emission, estimating the mechanical work that would be done on the photosphere by a sudden shift in magnetic inclination consistent with the magnetic signatures. They found values roughly consistent with energy estimates based on helioseismic observations.

It must be admitted that any mechanism that proposes to express flare acoustics in terms of any single one of these mechanisms would have to be a great oversimplification of the reality. Among detailed models of chromospheric waves driven by thick-target heating, only Allred *et al.* (2005) take back-warming into account. This may reduce radiative losses in waves generated by thick-target heating. Modeling efforts to date have yet to include an account of the inclined magnetic fields that dominate sunspot penumbrae, from which strong seismic emission has invariably emanated in instances we know of so far.

Donea *et al.* (2006b) and Moradi *et al.* (2007) published rough estimates of the energy in flare acoustic transients generated by sudden photospheric heating based on intensity images. These were roughly consistent with energy estimates based on the helioseismic observations they analyzed. However, these estimates are relatively crude and contain no account of penumbral magnetic fields.

[1] As in the rest of this study, "transient" refers to shifts on a time scale of order $\tau \sim 2H/c$ or shorter, where H is the density scale height of the solar atmosphere and c is the sound speed. This is approximately 40 seconds in the photosphere. It should be understood that the magnetic signatures actually observed are both transient and long-lasting. It is particularly the transient component that is understood to be relevant for the excitation of flare acoustic emission.

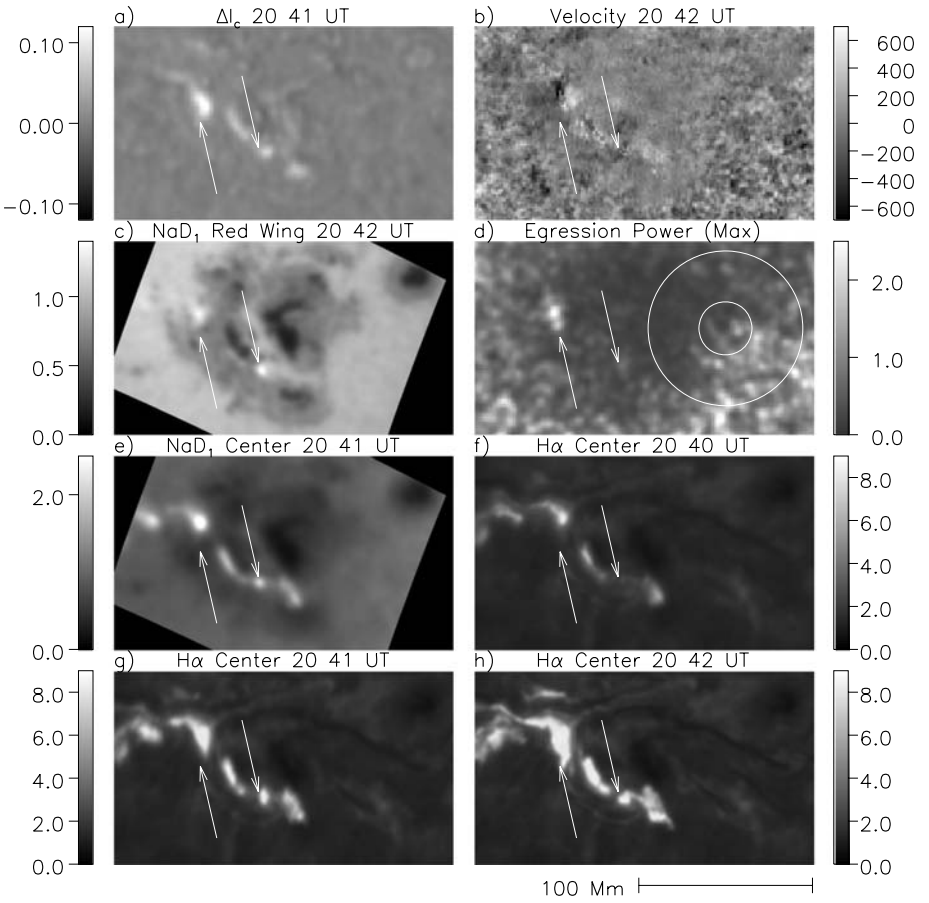

Figure 1 Co-spatial comparison of acoustic emission, Hα, Na D_1-line and continuum emission, and Doppler disturbance in AR 10486 in the impulsive phase of the flare of 29 October 2003, taken from Beşliu-Ionescu *et al.* (2007). Intensities are normalized to unity for the quiet Sun at disk center. (a) Difference between two visible-intensity images taken a minute before and a minute after the time indicated above the panel. (b) Transient downward Doppler disturbance (in meters per second) appearing in AR 10486 during the impulsive phase of the flare. (c) Emission in the red wing of the Na D_1 line, 0.14 Å from line center, showing compact downdrafts. Left and right arrows reproduced in all frames locate these for reference. (d) 5 – 7 mHz egression power map of AR 10486. The annular pupil of the egression computation is drawn at the right of this panel. (e) Impulsive-phase emission in the center of the Na D_1 line. (f) – (h) Line-center ISOON Hα images of AR 10486 at one-minute intervals beginning at 20:40 UT. Times are indicated above respective panels.

2. Mechanics of Seismic Emission Driven by Photospheric Heating

We review estimates by Donea *et al.* (2006b) and Moradi *et al.* (2007) of seismic emission driven by photospheric heating, referring to the diagram in Figure 2. In the exercise to follow we consider the transient energy flux that would result in a horizontally invariant, gravitationally stratified atmosphere if we could engage a massless piston at some depth (z_0) to apply a sudden, step-function increment (δp) in the pressure, initially p_0 at this depth, represented by step 1 in Figure 2. We suppose this excess to be maintained until the surface settles to a new static equilibrium, indicating that the transient driven by the resulting sud-

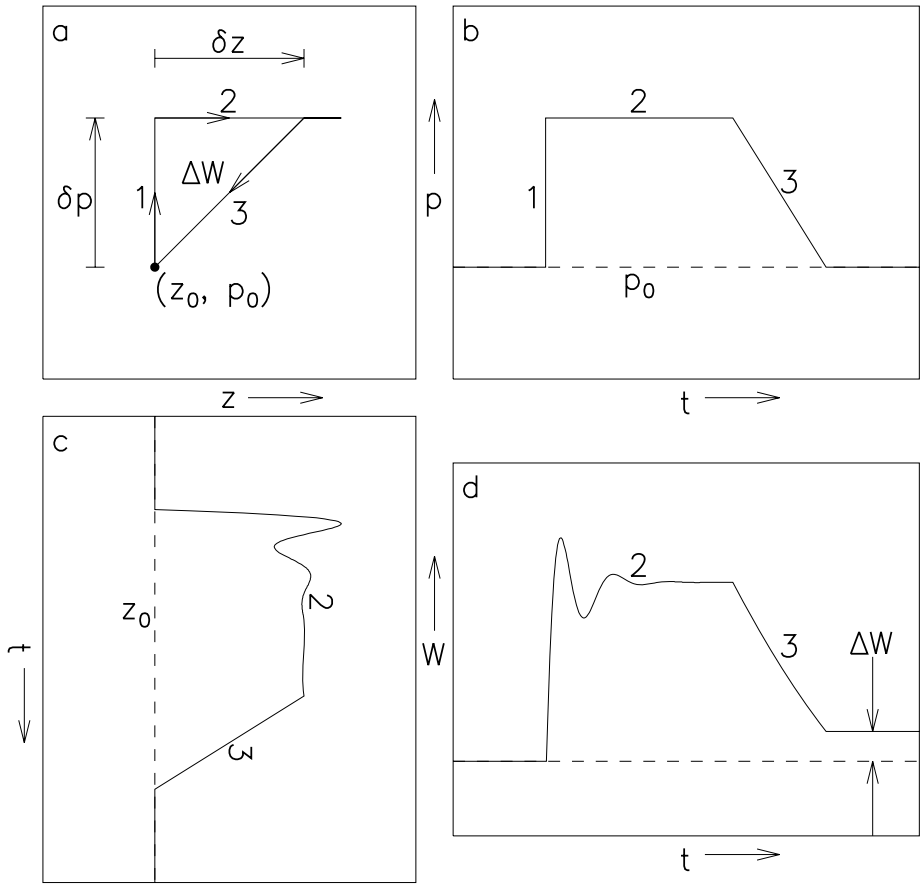

Figure 2 The pressure (frames a and b), vertical displacement (frames a and c) and work done (frame d) as a function of time (frames b – d) by a piston that introduces a sudden increment (δp) in pressure, initially (p_0), at depth (z_0) in a horizontally invariant, gravitationally stratified atmosphere (step 1 in all frames). The pressure increment is maintained while the transient driven by the resulting sudden impulse escapes downward into the medium (step 2). Once the piston has come to a displaced equilibrium, a quasi-static relaxation of the pressure back to that of the undisturbed medium is carried out (step 3). The work (ΔW) represented by the area of the triangular figure in frame a is equal to the energy carried away by the transient during step 2 of the cycle.

den impulse has escaped downward into the underlying medium, a development that occurs during step 2 in Figure 2. We now suppose that the depth ($z_0 + \delta z$) at which the piston eventually settles is that at which the pressure in the undisturbed atmosphere had previously been $p_0 + \delta p$. For a pressure increment that is a relatively small fraction of p_0, this would be accurately approximated by

$$\delta p = \rho g \delta z, \tag{1}$$

where ρ is the density of the solar medium and g is the gravitational acceleration in the neighborhood of z_0.

Finally, by quasi-statically relaxing the pressure to its initial value, a process represented by step 3 in the diagram, and equating the area (ΔW) of the resulting triangular hysteresis

loop that appears in Figure 2a to that which escapes in the transient, we find that

$$\Delta W = \frac{1}{2}\delta p \delta z = \frac{(\delta p)^2}{2\rho g}. \tag{2}$$

For a rough estimate of the pressure perturbation to be expected from sudden heating of the low photosphere, we proceed along lines somewhat parallel to Wolff (1972). Based on Boyle's law, we suppose that

$$\frac{\delta p}{p_0} = \frac{\delta T}{T_0}, \tag{3}$$

wherein the heating is expressed in terms of a characteristic temperature increase (δT) divided by a reference temperature (T_0) characterizing the preflare photosphere. It must be realized that even for an initially isothermal atmosphere Equation (3) can be an accurate representation of the mechanics only to within about a factor of two, since for it to accomplish a depression of the underlying medium requires the photosphere to expand, which results in a reduction in density. Moreover, such a pressure excess can only be maintained for a period comparable to the recoil time,

$$\tau_{\rm r} \sim \frac{2H}{c}, \tag{4}$$

of the heated layer, where H is the density e-folding height of the medium and c is the sound speed.[2] This is approximately 40 seconds in the low photosphere.

After Equation (3) of Wolff (1972), we approximate the heating associated with an excess ($\delta F_{\rm rad}$) in continuum flux by the Stefan – Boltzmann law:[3]

$$\frac{\delta T}{T_0} \sim \frac{1}{4}\frac{\delta F_{\rm rad}}{F_{\rm rad0}}. \tag{5}$$

It follows that the energy deposited into transient emission is

$$\Delta W \sim \frac{p_0^2}{32\rho_0 g}\frac{(\delta F_{\rm rad})^2}{F_{\rm rad0}^2}. \tag{6}$$

Donea *et al.* (2006b) and Moradi *et al.* (2007) found reasonable quantitative agreement between energy fluxes derived from egression power maps and Equation (6) applied to intensity observations from the Global Oscillation Network Group (GONG). However, the outstanding uncertainties are much too large to assure that anything like the entirety of the seismic emission measured is due to photospheric heating. This is not only because of the crudness of the hydrodynamics, including the neglect of magnetic forces, but also because of significant uncertainties in how concentrated the intensity distribution actually is. The

[2]This point is reinforced by bearing in mind that the pressure averaged over an extended time is the column mass density multiplied by g, which in a horizontally invariant geometry is unchanged by local heating of the medium. We note that $\tau_{\rm r}$ in Equation (4) is the reciprocal of $\omega_{\rm ac}$, the familiar acoustic cutoff frequency.

[3]The general accuracy of the approximation stated by Equation (5) rests on the close thermal connection between the photosphere and the ambient radiation field generally expressed by the term local thermodynamic equilibrium (LTE), a condition from which the overlying chromosphere deviates radically. Its accuracy in the photosphere depends on whether the continuum excess is a direct result of photospheric heating alone or the result of back-warming, in which case we understand $\delta T/T_0$ to be less by a factor of approximately two.

GONG images show this with limited resolution. For any given spatially integrated excess ($\delta F_{\rm rad}$) the integrated square-excess can be regarded as inversely proportional to the characteristic area from which the emission emanates. If this area is significantly less than the resolution of the observations, the transient would be proportionally more powerful than estimates based on the intensity maps.

If seismic emission from solar flares is substantially a result of photospheric heating, then Equation (6) explains why the energy delivered to the seismic transient is a small fraction of that which emanates from the region in the visible continuum, as indicated by the seismic energy estimates of Donea and Lindsey (2005). For purposes of general comparison we note that the energy flux carried by a propagating wave in a uniform medium is similarly proportional to the square of the velocity amplitude (v) of the motion of the medium,

$$F_{\rm ac} = \rho c v^2, \tag{7}$$

as the wave passes through it. This offers a basis for spatially detailed comparisons between holographic maps of acoustic emission and projections of the energy flux in acoustic transients driven by photospheric heating associated with excess continuum emission. This will be the subject of the next section.

3. The GONG Intensity Observations

3.1. General Description

We already have a considerable database of intensity observations during acoustically active flares by benefit of GONG (Donea and Lindsey, 2005; Donea *et al.*, 2006b; Moradi *et al.*, 2007). In previous analyses, the use of the GONG intensity observations has been limited to some degree by the effects of the terrestrial atmosphere, through which the GONG instruments must observe the Sun. The primary technical question this study confronts is how the major effects of the terrestrial atmosphere on helioseismic observations of active regions can be characterized and whether these can be substantially discriminated from those of actual brightness variations in active regions. We are convinced that such a discrimination can be accomplished to a highly useful degree.

The GONG observations are made in the photospheric line Ni I λ6768 Å. The GONG instruments make a single full-disk Doppler image, a full-disk line-of-sight magnetogram, and a full-disk intensity image with a cadence of one minute during clear weather.

The GONG intensity images represent radiation integrated over an approximately Gaussian passband whose FWHM is 0.75 Å centered on the line. The line itself has a FWHM of 0.011 Å and an equivalent width of 0.07 Å (Debouille, Roland, and Neven, 1973; Donea *et al.*, 2006b). In this study, we treat the GONG intensity observations as representative of the continuum, understanding that this is subject to errors to the extent that the equivalent width of the line varies with continuum-intensity variations. Comparisons between GONG intensity images of white-light flares and concurrent irradiance variations by SORCE/TIM show agreement to within approximately 20% if the GONG intensity excess is attributed to a variation in the local temperature of a blackbody spectrum at 6768 Å. Figure 10 of Donea and Lindsey (2005) shows this comparison for the X10-class flare of 29 October 2003.

The pixel size in the GONG intensity images is 2.5 arcsec. However, the spatial resolution of the observations depends significantly on atmospheric conditions, which can change perceptibly from one image to the next.

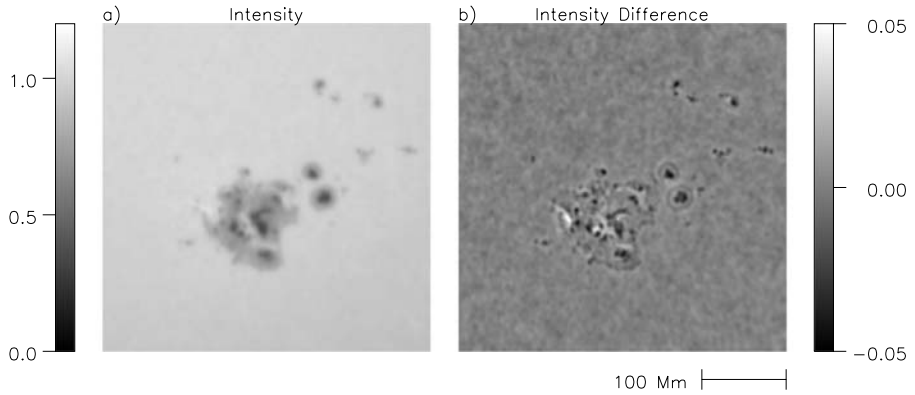

Figure 3 GONG intensity maps of AR 10486 on 29 October 2003. (a) The intensity at 20:42 UT, the impulsive phase of the flare. (b) The intensity difference between the map shown in the left frame and the intensity one minute earlier. The maps are normalized to unity for the quiet Sun.

3.2. Effects of Atmospheric Smearing

If the atmospheric smearing were independent of time, its effect on helioseismic measurements could be characterized simply in terms of limiting spatial resolution. Even with significant variations from one minute to the next, smearing does little in the quiet Sun in the way of introducing spurious temporal intensity variations. However, variable smearing of an active region with large *spatial* intensity variations introduces unacceptable spurious *temporal* variations. The character of these is illustrated in Figure 3. The left frame shows a intensity map of AR 10486 during the impulsive phase of the flare of 29 October 2003. The right frame shows the same intensity map but with the previous intensity map, one minute earlier, subtracted from it. For any particular pixel in the quiet Sun surrounding the active region, the intensity difference can be regarded as significantly representative of that which would have been observed if atmospheric smearing had undergone no change. However, within the active region, the difference manifested by a variation in the degree of smearing can easily predominate over true intensity variations. The result is a pattern in the intensity difference that reflects the morphology of the active region but flickers stochastically from one intensity difference to the next. This pattern can sometimes be minimized by selecting times at which the difference in the degree of atmospheric smearing was accidentally relatively small if not entirely null. The two-minute intensity difference represented in Figure 1a is a happy example of such an occurrence. However, routine helioseismic analysis cannot rely on such accidents, and this provides the motivation for the remedial exercise that follows.

3.3. Correcting Variations in Atmospheric Smearing

Among the many momentary effects terrestrial atmospheric turbulence is known to exert on astronomical images, two are particularly familiar: *i*) a local stochastic translation of the region of interest, which we will represent here by a vector displacement ($\boldsymbol{\alpha}$) in the image plane, and *ii*) a smearing of the image, such as that already discussed, which we will represent by a scalar parameter (β) whose character we will specify shortly. When the smearing is isotropic over the region of interest, moreover, the point spread function of the smearing has a finite upper bound with a characteristic radius that is significantly less than

the predominant scales of the source to be examined, and, finally, ($\boldsymbol{\alpha}$) is similarly less than the source scales; the effects of the smearing can be approximated by a field of the following form:

$$I'(\mathbf{r}) = I(\mathbf{r}) - \boldsymbol{\alpha} \cdot \nabla I(\mathbf{r}) + \beta \nabla^2 I(\mathbf{r}). \tag{8}$$

Here $I'(\mathbf{r})$ represents the intensity map of the translated and smeared source at location $\mathbf{r}$ in the image plane such that $I(\mathbf{r})$ would represent that of the un-smeared, untranslated source.

The characteristic lifetime of atmospheric scintillation is only a fraction of a second. For intensity maps integrated over many times this lifetime, during which the solar disk image is continually stabilized by limb tracking, $\boldsymbol{\alpha}$ averages to only a small fraction of what it could be for a single, instantaneous snapshot. This is the case for the GONG observations, in which each pixel represents radiation integrated for a full minute. The smearing that characterizes the integrated image might be significantly greater than for an instantaneous snapshot, but it is more likely isotropic. In any case, Figure 3 makes it clear that atmospheric smearing integrated over a full minute varies significantly from one minute to the next, and it is straightforward to confirm that the pattern that appears in Figure 3b conforms closely to some constant times the Laplacian of either of the two intensity maps from which the difference was computed.

In practice, what is more important than whether Equation (8) accurately represents the overall smearing introduced by the terrestrial atmosphere is that it can apply to just the variation in smearing. This can be represented by applying a relatively small-β differential smearing to an intensity map $[I(\mathbf{r})]$ that represents a source that has already been smeared by the atmosphere to a nominal degree that is constant. It then must simply be recognized that the differential smearing can be negative, meaning a differential resharpening of the image, which is accomplished by β itself being negative rather than positive.

The procedure we prescribe, then, is to adjust $\boldsymbol{\alpha}$ and β so as to optimize the fit of each image in the time series to a single reference image in a region that excludes that in which significant white-light emission actually occurs during the flare. The results of this clean-up operation is illustrated in Figure 4. In this case, the intensity in the right frame is the difference between the intensity shown in the left frame and preflare intensity averaged over

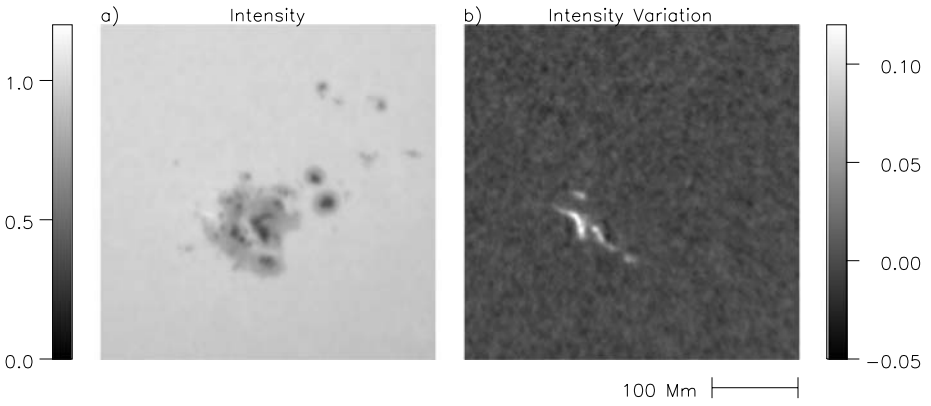

Figure 4 GONG intensity maps of AR 10486 normalized to unity for the quiet-Sun intensity and corrected for variations in smearing by the terrestrial atmosphere. (a) The intensity map shown in Figure 3a corrected for variable smearing. (b) The intensity difference between the map shown in Figure 4a and the preflare intensity averaged over a 300-second period similarly corrected.

a 300-second period. This image cleanly shows impulsive-phase emission from the active region that was relatively subtle in Figure 3.

With the intensity maps stabilized to this degree, it is now possible to apply essentially the same spectral-analysis techniques to GONG intensity observations of active regions as those applied to the MDI Doppler images for helioseismic applications. This is the object of the section that follows.

3.4. The High-frequency Spectrum of the Intensity

A careful comparison of the acoustic source distribution shown in Figure 1d with the distribution of intensity map shown in Figure 1a shows considerable excess radiation emanating from regions from which no significant seismic emission is detected. There are two major reasons for anticipating this:

1. To drive seismic emission, the heating must be sudden. The significant onset must be accomplished in a time not far in excess of the natural recoil time, $\tau_r \sim 40$ seconds [see Equation (4)], of the heated layer. The overwhelming preponderance of intensity excess from the flare of 29 October 2003 emanated from far outside of the acoustic source, but also on a time scale much longer than τ_r.
2. The efficiency of seismic emission driven by photospheric heating is greatly enhanced if the available heating flux is concentrated into a relatively compact region. This is simply because $(\delta F_{\rm rad})^2$ integrated over the solar surface is greater for a given $\delta F_{\rm rad}$ integrated over the same surface if the flux is concentrated into a smaller region. High-frequency seismic emission is proportional to the square of the sudden component of $\delta F_{\rm rad}$, which significantly emphasizes excesses that are more compact, spatially as well as temporally.

To address the issue of suddenness, we note that the range of characteristic times $\tau_c \sim 1/(2\pi\nu)$, for variations in the $5-7$ mHz spectrum are $32-23$ seconds, comfortably less than τ_r, qualifying heating in this part of the temporal spectrum as a prospective source of seismic emission. This may account in large part for the relative "hardness," of flare acoustic emission mentioned in the introduction, as compared with seismic waves produced by subphotospheric convection.

Motivated by this observation, we proceed by computing the power in the $5-7$ mHz intensity-excess from the smearing-corrected GONG intensity observations and comparing maps of this with concurrent maps of the acoustic-source power (*i.e.,* the egression power), of which Figure 1d shows the latter at seismic maximum. This exercise relies on the simple assumption that the relationship between the specific intensity (I_c) measured by GONG and the energy flux ($F_{\rm rad}$) integrated over the entire spectrum as applicable to photospheric heating is such that relatively small variations in the latter are linearly proportional to the former, and vice versa. The result, shown in Figure 5, is the subject of the discussion that now follows.

4. Discussion and Conclusions

Notwithstanding differences on a microscopic level, the morphologies of the $5-7$ mHz acoustic-emission and intensity-excess powers shown in Figure 5 are remarkably closely aligned. Figure 5 also graphically illustrates how high-frequency seismic emission driven by photospheric heating connected to excess visible-light emission can be relatively unresponsive to local excesses that are clearly seen in individual GONG images if these are insufficiently concentrated spatially or insufficiently sudden. This is why the brightest kernels in

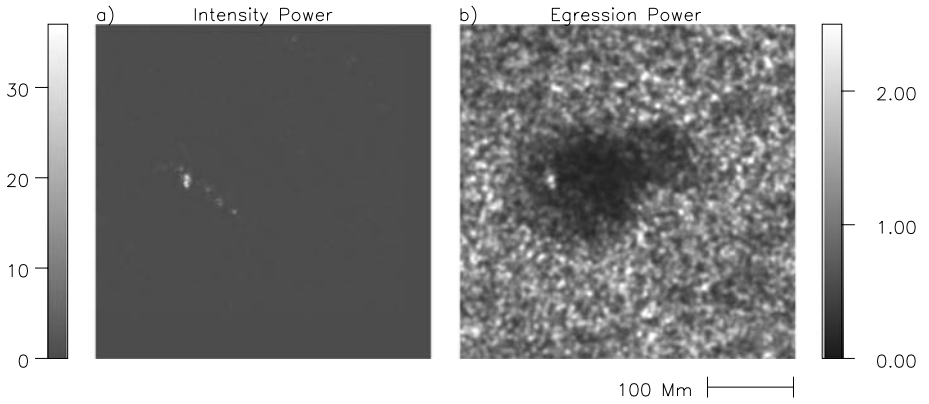

Figure 5 Comparison between 5 – 7 mHz intensity-excess power (a) and holographic egression power (b) maps for the flare of 29 October 2003. The intensity-excess power is derived from GONG observations corrected for variable smearing by the terrestrial atmosphere, as described in the text. The intensity-excess power is expressed in millionths of the square of the quiet-Sun intensity. The egression power is normalized to a mean of unity for the quiet Sun.

Figure 1a are so heavily represented in Figure 5a and hence, we suppose, in high-frequency seismic emission.

In fact, somewhat similar behavior can be expected to apply to magnetic-force transients (Hudson, Fisher, and Welsch, 2008), which we have not properly begun to consider in this study. Donea *et al.* (2006b) express concern about the accuracy of magnetic measurements made in the radiative environment of a white-light flare. We understand that shifts in the radiative environment during a white-light flare can spuriously introduce a significant shift, even possibly a reversal, in line-of-sight magnetic signature (Patterson, 1984). Other analysts acknowledge this concern but note that the magnetic signature often remains shifted for some time after the impulsive phase, when the radiative environment has relaxed to something like the preflare values. Donea *et al.* (2006b) express a concern that molecular contamination in the sunspot spectrum may affect magnetic signatures. If the molecular abundances of the photosphere are perturbed by excess continuum and UV radiation during the impulsive phase of the flare, it is not entirely clear how long it should take for molecular balance to recover after the impulsive phase of the flare. This is a particular concern for molecules whose atomic components are many times the mass of hydrogen and orders of magnitude less abundant.[4] Our understanding of this would benefit from spectral observations of an active region in appropriate molecular lines in the hour or so succeeding a white-light flare. This would be just one of a possibly significant number of useful applications for a white-light flare alarm that could be provided by the Helioseismic-Magnetic Imager (HMI) onboard the *Solar Dynamics Observatory* in solar activity cycle 24.

A comparison between Donea and Lindsey (2005) and Sudol and Harvey (2005) suggests that magnetic-transient signatures do not always exactly coincide with excess visible-light emission. This suggests that a careful spatial comparison benefiting from the local discrimination that high-frequency holographic observations can deliver may discriminate magnetically driven transient emission from that resulting from photospheric or chromospheric heat-

[4]Some authorities regard this to be improbable, as most molecular lines in sunspot penumbrae, from which most white-light flares and transient acoustic emission emanate, are much weaker than in sunspot umbrae.

ing. What is needed for such a discrimination is simultaneous high-quality Doppler-seismic, Stokes-magnetic, and visible-continuum observations of acoustically active flares.

A major obstacle to helioseismology from its inception has been the relative sparcity of controls, in that the object of study is mostly hidden from view in the electromagnetic spectrum, and the means of viewing it acoustically, for the most part, has yet to be developed. Four prospective sources of acoustic waves in the solar interior have been considered since the advent of helioseismology: *i*) convection (Goldreich and Keeley, 1977b), *ii*) overstable oscillations (Ando and Osaki, 1975; Antia, Chitre, and Kale, 1977; Goldreich and Keeley, 1977a), *iii*) comets occasionally plunging into the Sun (Kosovichev and Zharkova, 1995), and *iv*) flares (Wolff, 1972; Haber, Toomre, and Hill, 1988; Kosovichev and Zharkova, 1995). Of these, only flares can substantially be seen in the electromagnetic spectrum above the photosphere. The discovery of seismic emission from flares thus presents local helioseismology with an exceptionally useful prospective control resource. What is needed to develop this resource to its full potential is detailed modeling of how acoustic transients are generated, how they propagate through the outer solar atmosphere, and how they are injected into the solar interior, with a careful account of non-LTE radiative transfer and Lorentz forces in inclined magnetic fields and a realistic assessment of their observational manifestations.

Acknowledgements This research has benefited greatly from time and resources contributed by D. Beşliu-Ionescu, H. Moradi, J. Martinez-Oliveros, and P.S. Cally. We greatly appreciate the insight of the anonymous referee. This research was supported by grants from the Astronomy and Stellar Astrophysics Branch of the US National Science Foundation.

References

Allred, J.C., Hawley, S.L., Abbett, W.P., Carlsson, M.: 2005, *Astrophys. J.* **630**, 573.
Ando, H., Osaki, Y.: 1975, *Pub. Astron. Soc. Japan* **27**, 518.
Antia, H.M., Chitre, S.M., Kale, M.: 1977, *Solar Phys.* **56**, 275.
Beşliu-Ionescu, D., Donea, A.-C., Mariş, G., Cally, P., Lindsey, C.: 2007, *Adv. Space Res.* **40**, 1921.
Debouille, L., Roland, G., Neven, L.: 1973, *Spectrophotometric Atlas of the Solar Spectrum from λ3000 to λ10000*, Inst. d'Astrophysique, Liège.
Ding, M.D., Fang, C.: 1994, *Astrophys. Space Sci.* **213**, 233.
Donea, A.-C., Lindsey, C.: 2005, *Astrophys. J.* **630**, 1168.
Donea, A.-C., Braun, D.C., Lindsey, C.: 1999, *Astrophys. J.* **513**, L143.
Donea, A.-C., Besliu-Ionescu, D., Cally, P.S., Lindsey, C.: 2006a, In: Uitenbroek, H., Leibacher, J., Stein, R. (eds.) *Solar MHD: Theory and Observations – a High Spatial Resolution Perspective*, *CS*-**354**, Astron. Soc. Pac., San Francisco, 204.
Donea, A.-C., Besliu-Ionescu, D., Cally, P.S., Lindsey, C., Zharkova, V.V.: 2006b, *Solar Phys.* **239**, 113.
Fisher, G.H., Canfield, R.C., McClymont, A.N.: 1985, *Astrophys. J.* **289**, 434.
Goldreich, P., Keeley, D.A.: 1977a, *Astrophys. J.* **211**, 934.
Goldreich, P., Keeley, D.A.: 1977b, *Astrophys. J.* **212**, 243.
Haber, D.A., Toomre, J., Hill, F.: 1988, In: Christensen-Dalsgaard, J., Frandsen, S. (eds.) *Adv. Helio- and Asteroseismology*, *IAU Symp.* **123**, Kluwer, Dordrecht, 59.
Hudson, H.S., Fisher, G.W., Welsch, B.J.: 2008, In: Howe, R., Komm, R., Balasubramaniam, K.S., Petrie, G.J.D. (eds.) *Subsurface and Atmospheric Influences on Solar Activity*, *CS*-**383**, Astron. Soc. Pac., San Francisco, 221.
Kosovichev, A.G.: 2006, *Solar Phys.* **238**, 1.
Kosovichev, A.G.: 2007, *Astrophys. J.* **670**, L65.
Kosovichev, A.G., Zharkova, V.V.: 1995, In: Hoeksema, J.T., Domingo, V., Fleck, B., Battrick, B. (eds.) *Helioseismology*, *Proc. 4th SOHO Workshop* **SP-376**, ESA, Noordwijk, 341.
Kosovichev, A.G., Zharkova, V.V.: 1998, *Nature* **393**, 317.
Lindsey, C., Braun, D.C.: 2000, *Solar Phys.* **192**, 261.
Martinez-Oliveros, J., Moradi, H., Donea, A.-C.: 2000, *Solar Phys.* **192**, 261.

Moradi, H., Donea, A.-C., Lindsey, C., Besliu-Ionescu, D., Cally, P.S.: 2007, *Mon. Not. Roy. Astron. Soc.* **374**, 1155.
Patterson, A.: 1984, *Astrophys. J.* **280**, 884.
Sudol, J.J., Harvey, J.W.: 2005, *Astrophys. J.* **635**, 647.
Wolff, C.L.: 1972, *Astrophys. J.* **176**, 833.
Zharkova, V.V., Kosovichev, A.G.: 2002, In: Wilson, A. (ed.) *From Solar Min to Max: Half a Solar Cycle with SOHO*, *Proc. SOHO 11 Symposium* **SP-508**, ESA, Noordwijk, 159.